Fine-particle magnetic oxides

1993 J. Phys.: Condens. Matter 5 8487

(http://iopscience.iop.org/0953-8984/5/45/002)

J. Phys.: Condens. Matter 5 (1993) 8487–8508. Printed in the UK

REVIEW ARTICLE

Fine-particle magnetic oxides

Q A Pankhurst† and R J Pollard‡

† Department of Physics, University of Liverpool, Liverpool L69 3BX, UK
‡ Department of Physics, Monash University, Clayton, Victoria 3168, Australia

Received 22 June 1993, in final form 3 September 1993

Abstract. The response of fine-particle magnetic oxides to applied magnetic fields is of primary importance in several areas of applied physics, such as magnetic separation, magnetic fluid devices, and magnetic recording. It is also of fundamental interest. In this article contemporary research on the important properties of magnetic oxide particles is reviewed, including both applied and basic work. The microscopic and macroscopic properties of ferrimagnetic and antiferromagnetic fine-particle systems are considered. Special attention is paid to the physics of magnetization reversal mechanisms, surface effects, and the intrinsic properties of fine-particle magnetic oxides.

Contents

1. Introduction

There are a surprising number and variety of areas in daily life in which the behaviour of

0953-8984/93/458487+22$07.50

fine-particle magnetic oxides in response to a magnetic field is of fundamental importance†. This is partly due to the ubiquity of fine-particle magnetic oxides in naturally occurring forms, and partly due to the special properties of finely subdivided materials which lead to their widespread utilization in manufactured forms. Examples include the chains of magnetite particles found in magnetotactic bacteria; the several grams of iron that is stored in the human body as the ferrihydrite cores of iron-storage proteins; the magnetic phases and weathering products often found on rocks, soils, and coals; the magnetite particles used in magnetic fluids for sealing, damping, sensing, and bearing applications; and the maghemite, barium ferrite, and chromium dioxide particles used in computer hard and floppy disks, credit cards, and audio and video recording tapes.

Finely subdivided particles can exhibit special properties that differ from those of the bulk material. An important example arises in ferrimagnets, where below a critical size, fine particles may contain only a single magnetic domain. This results in a large magnetic moment per unit volume, and a large magnetic anisotropy. The large magnetization is an advantage for applications that rely on a strong response to an applied field, such as magnetic-fluid devices and recording media. The large anisotropy presents an energy barrier to the process of magnetization reversal, as undertaken during the writing of recording media, and in the ambient state determines the stability of the recorded data.

Other special properties include the effects of the relatively high surface-to-volume ratio, and the related effect of particle coating, which in some cases can dramatically alter the magnetic properties of the base material. In the limit of very small particle sizes, long-range magnetic order may break down, and the effects of lattice vacancies and other anomalies become prominent. In ultrafine particles of antiferromagnets a small net moment becomes apparent because of an imbalance in the numbers of oppositely directed moments.

The significance of many fine-particle magnetic oxides stems from their behaviour in an applied magnetic field. In magnetotactic bacteria, chains of magnetite particles act as compass needles, causing the bacteria to orient and swim along geomagnetic field lines, and thereby distinguish between up and down—an otherwise difficult task for bacteria of insignificant mass. In magnetic separation and filtration applications, the force exerted on the particles by a non-uniform magnetic field allows phases to be separated. In magnetic recording media, the signal-to-noise ratio, the density of information storage, the speed of reading and writing etc depend intimately on the magnetic properties of particles on a substrate and on the response to a magnetic recording head.

In this article an overview of the response of fine-particle magnetic oxides to applied fields is presented. The aim is to highlight recent advances in experiment and theory in the context of applications, without losing sight of the objectives of contemporary research. The impetus for such research is twofold. First, it is a component of the research and development programs of the manufacturers of those products that utilize fine magnetic particles. Second, it is undertaken by independent scientists whose aim is to better understand the physical principles governing the behaviour and properties of particulate matter. These two strands of research are closely related, as the particles that exhibit the most interesting physical phenomena are often those that are manufactured for commercial purposes. A better understanding of the physics of fine-particle magnetism can lead to new and improved industrial applications.

† In this context the term 'fine particle' refers to particles with size dimensions on the micrometre or nanometre scale, and 'magnetic oxide' refers to the ferrimagnetic and antiferromagnetic oxides (and in some cases oxyhydroxides) of the magnetic transition metals such as Fe, Co, and Ni. Superconducting materials are not included.

The structure of this article is as follows. First, the objectives of contemporary application-oriented research on fine-particle magnetic oxides are reviewed, focusing on the areas of magnetic fluids, separation and filtration, magnetic recording, and applications in biology and medicine. Thereafter, several distinct areas of fundamental research are reviewed: magnetization reversal mechanisms, surface effects, and the intrinsic properties of fine particles. Finally, some comments are made regarding the prospects for further progress in research on fine-particle magnetic oxides.

2. Application-oriented research objectives

To place in context those aspects of current research that are application oriented, we consider important industrial and biological applications in which the response of fine-particle magnetic oxides to an external magnetic field plays an integral part. In the following, brief descriptions of the applications in question are presented, and the requirements that those applications place on the fine-particle systems are noted. The areas of fundamental research that are pursued in order to improve or refine the applicability of the fine-particle system are then described.

2.1. Magnetic fluids

Magnetic fluids, or 'ferrofluids,' are generally based on either the ferrimagnetic oxide magnetite (Fe_3O_4), or on the ferromagnetic metals Fe or Co. The magnetite-based fluids consist of submicrometre particles of Fe_3O_4 suspended in either an organic or inorganic liquid (e.g. kerosene or water), or an oil (e.g. synthetic esters or hydrocarbons). The choice of carrier liquid depends on which fluid dynamical properties are required.

2.1.1. Engineering applications. The engineering applications of magnetic fluids have been reviewed by several authors [1–3]. The most common application is in O-ring seals, where a combination of permanent magnets and pole pieces are arranged so that narrow regions of intense magnetic field retain the fluid as distinct rings around a rotating shaft (see figure 1). This provides a leak-tight seal, which has the low friction of an oil bearing but with superior heat-transfer characteristics. Seals with the ability to maintain integrity under vacuums of 10^{-8} Torr and with surface speeds at the fluid–shaft interface of up to 10 m s^{-1} have been constructed. Such seals are appropriate in devices such as lasers, continuous-operation x-ray tubes for CAT scanners, Winchester-type magnetic memory disk drives, and sputtering systems used in semiconductor processing.

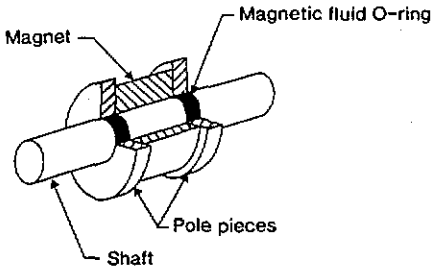

Figure 1. Schematic diagram of a magnetic-fluid O-ring seal around a rotating shaft.

Research on magnetic fluids for engineering applications focuses on understanding and modelling the electrostatic and magnetic interparticle interactions in the fluid, and the related questions of the effect of surfactant coatings. The intrinsic stability of both the magnetic particles and the carrying fluid in response to both high temperature and pressure is also an important factor, as is the manner in which any such effect might alter the inherent fluid dynamics of the system.

2.1.2. Magnetic imaging. Another use of magnetic fluids is in the Bitter method of magnetic imaging. The two main commercial applications are in the quality control of magnetic recording media, and in the identification of structural defects in massive steel structures. In the magnetic-recording industry, a water- or organic-based fluid carrying ~ 70 Å magnetite particles is spread on the recording disk or tape. The magnetite particles are attracted to the regions of maximum field under the influence of the field gradients of the domain walls, and thus congregate at the domain boundaries. The use of the fine particles allows the resolution of individual bits, which are ~ 2 μm wide. (A conventional Bitter-method fluid comprises ~ 1 μm sized particles.) Further improvement in resolution may be obtained by using scanning electron or tunnelling microscopes, rather than optical microscopes, to image the particles on the surface [4, 5].

In the oil and gas industries, a suspension of magnetite particles in paraffin or water is sprayed onto the transversely magnetized surface of structural components. Any cracks in the surface, provided that they do not run parallel to the magnetizing direction, result in a leakage field above the surface, which in turn attracts the magnetite particles and makes the defects visible to an operator (see figure 2). This technique of non-destructive testing, known as 'magnetic particle inspection', is of particular relevance to safety control, since most load failures are located in the region of surface defects. Magnetic particle inspection is something of a 'black art' relying heavily on operator experience. Only recently have techniques been developed that offer the potential of reproducible and controllable performance [6–8].

In developing magnetic fluids for use in imaging applications, research is primarily directed towards understanding the physics of the interactions between particles and the magnetized surfaces of massive objects. This includes modelling the force on a fine magnetic particle for different surface crack morphologies, the special properties (e.g. large field gradients) of open defects, and establishing estimates of the probability of detection as a function of particle size and other factors. Consideration is also given to the effects of particle surfactants, such as the fluorescent pigments that are sometimes used to enhance the visiblity of features, and to time-dependent effects, such as the response time of a magnetic fluid to an alternating applied field.

2.2. Separation and filtration

Applications utilizing the effect of applied fields on fine particles to achieve filtering and phase separation are widespread in the mineral processing industry [9]. In the early days very simple magnet structures were used to extract strongly magnetic minerals rich in iron. Over the last twenty years the technology has developed largely through the employment of both high-field-intensity and high-field-gradient separators [10–13]. These are now used on a commercial scale to separate micrometre sized materials even if they are only feebly magnetic.

Several distinct separation technologies are currently either in use or undergoing development, for both wet and dry applications. These include high-gradient magnetic

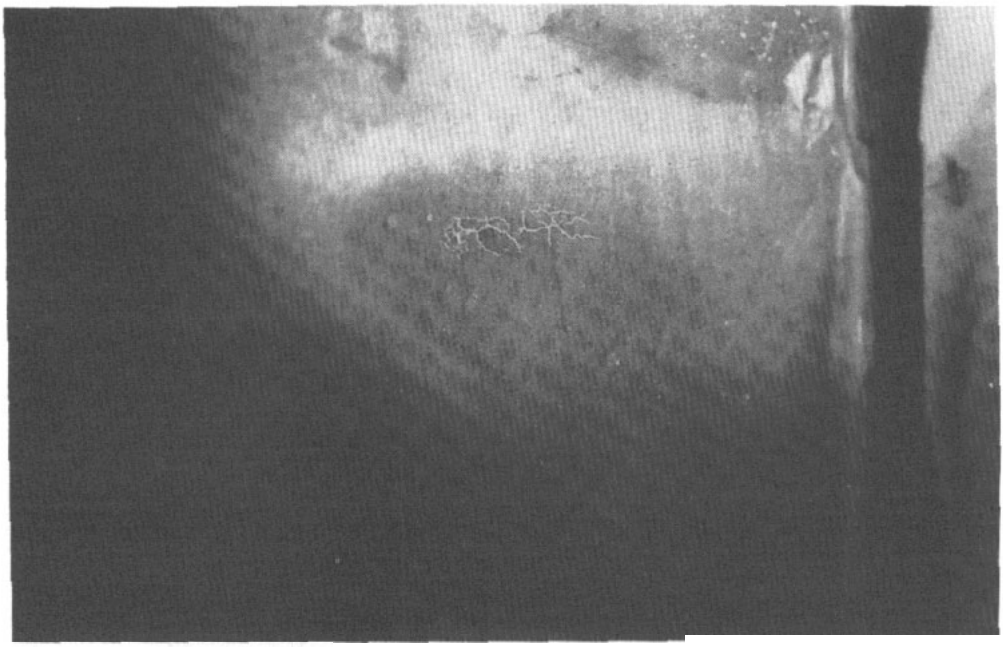

Figure 2. Surface cracks in an automobile crankshaft made visible under ultraviolet light using $\leqslant 5$ μm magnetite particles coated with a fluorescent resin. Photograph supplied by D G Lovejoy of Castrol (UK) Limited.

filtration and separation, open-gradient magnetic separation, separation in magnetically stabilized fluidized beds, and field-induced flocculation in fluids.

In high-gradient magnetic separation (HGMS) a suspension of particles in a liquid is passed through a stainless-steel wire mesh in a homogeneous background field of sufficient magnitude to saturate the magnetization in the wires (see figure 3). Regions of high field and field gradient (i.e. high $H\nabla H$) are established, attracting any magnetic particles towards the wires. In a typical filtering system steel wool of ~ 10 μm diameter (either bundled wires or randomly packed) in an external field of intensity $\sim 10^7$ A m^{-1} is capable of capturing particles of diameters in the range 1–100 μm from a fluid flowing at a rate of up to ~ 10 cm s^{-1}. The particles thus captured can be collected by simply switching off the external field and flushing the mesh with distilled water. Recent experiments have been performed on filters comprising stainless-steel beads rather than a wire mesh [14, 15]. Using spheres ranging in diameter from 50 to 200 μm, Haque *et al* [15] succeeded in filtering 65 nm α-Fe_2O_3 particles from an aqueous suspension flowing at 3 cm min^{-1}. This ability to capture submicrometre particles using a simple, inexpensive and easily constructed filter is a promising development.

Open-gradient magnetic separation (OGMS) is based on particle deflection rather than particle capture. The method offers the advantage of continuous operation, and can be used for either dry or wet streams of matter. In dry-particle OGMS, sometimes known as the 'falling-curtain' method, a stream falls under gravity either through the centre of a cylindrical Helmholtz split-pair solenoid, or on either side of the faces of a linear periodic array of magnets [16–19]. The applied field produces a lateral deflection force on the falling particles, and magnetic fractions are selectively drawn from the stream.

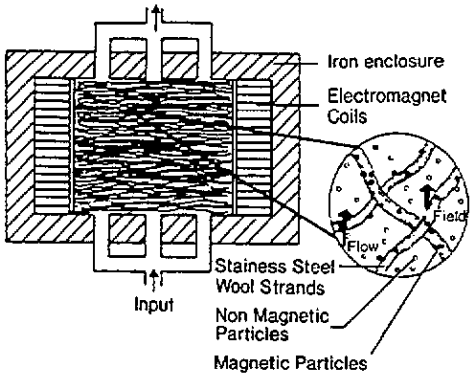

Figure 3. Cross section of a high-gradient magnetic filter. A slurry is forced through a stainless-steel wire mesh. The high magnetic field and gradient attracts any magnetic particles in the slurry to the mesh, while the non-magnetic particles are not affected and pass through the filter.

The properties of magnetic fine particles may also be used to facilitate the separation of non-magnetic particles according to their size and density. In a conventional separation process known as 'fluidization', a stream of compressed air is forced up through a container of dry particles at a pressure sufficient to allow the state in which the most dense particles fall to the bottom of the container [20]. A difficulty is that the fluidized state is often unstable. However, this may be alleviated by introducing magnetite particles to the filtering bed, and applying an external magnetic field of an appropriate strength to stabilize the fluidized state [21,22]. The resulting system is known as a 'magnetically stabilized fluidized bed'.

In both HGMS and OGMS the magnetic particles in liquid suspension are passed through the separator in a continuous stream. In contrast, the process of flocculation relies on field-induced interparticle aggregation to achieve separation [23]. Here the fluid may be at rest. The effect of an applied field, brought into contact with the walls of the containing vessel, is to induce aggregation. The local density increases to the extent that the aggregate settles out of the solution under the force of gravity.

There are two areas of fundamental research that are relevant to magnetic separation applications. The first relates to the physics of interparticle interactions, and in particular to the mechanism and requisite conditions for agglomeration and aggregation. The second relates to the intrinsic magnetic properties, especially the net magnetization, of different magnetic species as a function of particle size, morphology, crystallinity and temperature. An accurate identification of these intrinsic properties is necessary for an understanding of magnetic separation processes.

2.3. Magnetic recording

Ever since the 1900s, when Valdemar Poulsen invented a 'magnetic speech recorder' that used steel piano wires as a recording medium, advances in recording technology have continued unabated. Many books and reviews have been written about these developments [24–31]. The advent of high-density recording systems and high-quality particulate recording media has contributed greatly to the proliferation of computer-based systems.

The recording medium must have a large remanent magnetization for a strong signal on play-back and a moderate coercivity (sufficiently large to avoid inadvertent erasure but sufficiently low to enable writing at modest field strengths). Ideally the hysteresis loop will be 'square', with the remanent magnetization similar to the saturation magnetization. The elementary magnetic grains or particles need to be physically small and magnetically independent to enable short-wavelength recording, but not so small as to exhibit superparamagnetism. These prerequisites are met by only two types of medium: particulate dispersions of γ-Fe_2O_3, Co-modified γ-Fe_2O_3, CrO_2 or barium ferrite, or thin

metallic films of Fe or Co–Fe. For example, submicrometre γ-Fe_2O_3 particles have a saturation magnetization $M_s \simeq 340$ kA m^{-1} at room temperature, and a coercivity H_c in the range 20–28 kA m^{-1}.

Additional requirements for suitable particulate media are that the particles be well oriented, uniformly dispersed, and have a high packing fraction. A typical γ-Fe_2O_3 particulate dispersion contains 0.3 μm long acicular particles of 5:1 axial ratio, packed at a volume fraction of 40% in a flexible organic layer of thickness 2 μm for disks, and of thickness 5 μm for tapes. During recording, the magnetization of single-domain units is switched between two stable directions. Fields of four or five times the coercivity of the particles are required to saturate the magnetization in the desired direction. A schematic diagram of a transition region on the surface of a particulate recording medium is shown in figure 4.

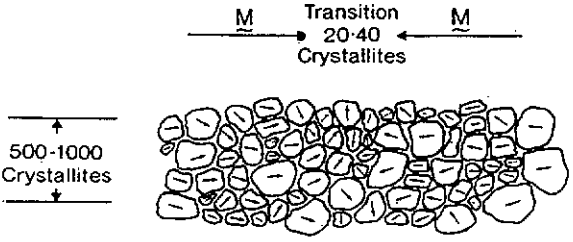

Figure 4. Schematic diagram (not to scale) of the transition region between two oppositely magnetized regions in a recording track. The small arrows represent the magnetization directions within individual particles.

Over the years there has been an ongoing effort aimed at improving the information-storage capacity of magnetic recording systems. Many different types of medium have been developed, such as 'thin-film' recording media in which the magnetic constituents are either sputtered or vacuum deposited onto the substrate [31], and 'perpendicular' recording media in which the preferred magnetization direction of the magnetic particles is perpendicular to the plane of the medium [32]. Fundamental research is centred on probing the intrinsic properties of the particles themselves, such as the dependence of magnetization on size and morphology, the effect of surface coatings (as in Co-modified maghemite) on magnetization and coercivity, and determinations of the magnetocrystalline anisotropies of ultrafine particles. Research is also directed at investigations of the magnetization reversal mechanisms in both isolated particles and particle assemblies, and the effect that interparticle interactions within the solid pigment dispersion might have on magnetization reversal.

2.4. Biology and medicine

Magnetite particles formed as biochemical precipitates have been identified in three of the five animal kingdoms [33], and are best known as the navigational 'compasses' found in magnetotactic bacteria [34]. For orientational purposes, the magnetite particles are single-domain crystals arranged in a chain (a magnetosome). This chain acts as a bar magnet and is oriented by the geomagnetic field; movement is therefore along the earth's flux lines. For low-mass organisms this method of attaining uniaxial movement may be more effective than gravitational orientation. For organisms of larger mass, such as European eels, biological sensors are required to detect the magnetic force and transfer the information to the nervous system. Most recently, magnetite and maghemite (substituted with Ti) have been found in the human brain, with crystal morphologies and structures resembling those precipitated by bacteria and fish [35]. The crystals occur in clumps of between 50 and 100 particles, and the particle sizes range up to 600 nm in diameter (within the single-domain limit).

Since their discovery over a decade ago, magnetotactic bacteria are finding a range of applications. They have been coated onto transformer sheets for domain imaging [36] and give useful information for rock magnetism and palaeomagnetism by acting as 'biomagnetometers' [37]. Their ability to ingest or precipitate ion species, and to be subsequently removed *via* a magnetic separator, provides a means of extracting heavy metals [38,39]. Their magnetite particles have been isolated for uses in enzyme immobilization [40].

Magnetic particles have numerous medical uses. Magnetite particles can act as a contrast agent for magnetic resonance imaging [41,42] and can be used for cell separation [43,44] and in various cancer treatments [45,46]. Chromium dioxide particles are used as the solid support in enzyme immunoassay [47]. Magnetic powders have also been used to orient biological assemblies [48] and to isolate red blood cells [49]. Cancer treatment may be performed by directing magnetite to tumour sites using a tubular implant (a liquid suspension comprising ultrafine magnetite particles surrounded by chains of dextran, a blood-plasma substitute) [50]. Localized heating of the magnetite by an RF generator then induces hypothermia in the targeted cells.

A 'laser magnet immunoassay' method has been developed for the sensitive detection of viral antigens [51]. Target viruses react with antibodies labelled with magnetite particles, and are subjected to a magnetic field. The antigens are attracted to one point on the surface, resulting in the lifting up of a small surface area which is detected *via* an interferometer. Very low concentrations of antigens can be detected, such as five particles of influenza virus and 0.1 pg ml^{-1} of human immunodeficiency virus antigen in human serum.

In these biological and medical applications one requires specific knowledge of the way in which a fine-particle system responds and behaves when the particles are in contact with organic matter. This includes models of intracellular particle motion, wherein all relevant forces, viz. thermal, elastic, and cellular, are considered [52]. Other questions relate to the physical properties of the particles themselves, especially such factors as the degree of magnetic or structural disorder, the onset of superparamagnetic behaviour, and, at a very fundamental level, the biomineralization process by which the fine-particle magnetic oxides are formed within the organism.

3. Fundamental research

Given the high level of both academic and manufacturing interest in the physical properties of fine-particle magnetic oxides, it is not surprising that a large research effort is directed towards studies of particulate systems. In the following we outline areas in which the research is concentrated.

3.1. Magnetization reversal

As information storage technology advances, and as the bit densities in magnetic recording media increase and the dimensions of the magnetic particles or grains decrease, research on the fundamental magnetization reversal process is becoming increasingly relevant [53–55]. In general the correlation between experimental and theoretical work is imperfect. The most precise theoretical micromagnetic modelling of the reversal process deals with isolated single-domain particles, but experimentally it is very difficult to isolate and study individual particles. Similarly, most experimental work deals with particle assemblies and dispersions. Although the theoretical modelling of such assembles is sophisticated, it is not as rigorous as for isolated particles.

3.1.1. Isolated particles. The simplest magnetic system for considering the process of magnetization reversal is a single-domain ferromagnetic or ferrimagnetic particle with uniaxial magnetic anisotropy. It is assumed that the particle is totally isolated so that interparticle interactions may be neglected. If an applied field $\boldsymbol{H}$ is directed antiparallel to the direction of magnetization $\boldsymbol{M}$, the state in which $\boldsymbol{M}$ is parallel to $\boldsymbol{H}$ becomes energetically favourable, and the initial state becomes metastable. The critical field strength required to overcome the magnetic anisotropy and to irreversibly change the magnetization of the particle is called the 'switching field', H_s. Here, for $\boldsymbol{H}$ collinear with the easy anisotropy axis, H_s has the same value as the 'coercivity' H_c, where H_c is the field at which the magnetization of the system falls to zero. In general, such as when $\boldsymbol{H}$ is not collinear with the easy axis, H_c and H_s do not necessarily coincide.

One question that may be asked regarding the reversal mechanism is whether the atomic moments in the particle move in unison. It is intuitively reasonable to look for 'cooperative' reversal modes in which the rotation of the individual moments begins and proceeds uniformly over the whole particle. For a particle shaped like an ellipsoid of revolution, it has been proved analytically that there are only three physically possible modes of cooperative reversal, namely 'coherent rotation', 'curling', and 'buckling' [56–58]. In the coherent rotation mode all the moments in the particle remain collinear throughout the reversal process [56]. In the curling mode the moments retain cylindrical symmetry about the major axis of the spheroid, but are not all collinear [58]. This may be envisaged as the moments on the surface of the spheroid responding to the applied field more freely than do the moments in the core. The buckling mode is rather complex, and is only applicable to elongated prolate spheroids with aspect ratios exceeding 5:1. It is generally thought to be an insignificant intermediary between the coherent rotation and curling modes [53, 58].

A schematic diagram illustrating the coercivity associated with the coherent rotation and curling modes for a prolate spheroid is given in figure 5. The coercivity is plotted as a function of the angle between the applied field and the easy anisotropy axis of the particle.

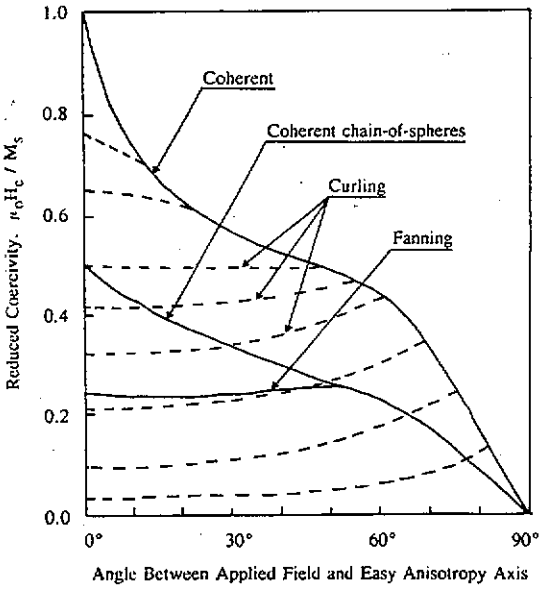

Figure 5. Schematic diagram of the reduced coercivity $\mu_0 H_c/M_s$ of an isolated particle as a function of the angle θ between the applied field and the easy anisotropy axis, where $\theta = 0$ corresponds to the field being aligned antiparallel to the net magnetization direction. Several modes of magnetization reversal are illustrated.

In general, analytic expressions for the reversal process have only been derived for

simple geometric cases, such as the spheroid and the infinite cylinder of circular or rectangular cross section. However, a successful model has been used to describe the reversal process in acicular particles, such as γ-Fe_2O_3, in terms of a 'chain of spheres' [57]. In this model it is assumed that a magnetostatic interaction occurs between the spheres, but no exchange interaction. Two reversal modes are predicted, a coherent rotation mode and a 'fanning' mode. In the fanning mode the moments reorient while remaining in a plane perpendicular to the applied field direction, with the sense of the rotation alternating from one sphere to the next along the chain. Both this mode and the coherent rotation mode have a smaller coercivity than in a prolate spheroidal particle of similar dimensions (see figure 5).

In the original formulation of the chain-of-spheres model it was assumed that the spheres possessed no magnetocrystalline anisotropy, so that the magnetic anisotropy was determined by the chain shape alone. The effect of crystalline anisotropy has recently been incorporated into the model, and appears quite significant in certain cases [59]. Also, the effect of having a compacted chain has been studied, where the spheres have planes of contact rather than points of contact [60]. For both the coherent rotation and fanning modes of reversal, the critical fields were found to increase as the contact area increases.

An alternative to a cooperative model of the reversal process is a 'nucleation' model, in which the reversal is at first localized, before spreading to the remainder of the particle. (This should not be confused with the term 'nucleation field', which denotes the field at which magnetization reversal begins to take place, irrespective of whether the reversal is cooperative. Nor should it be confused with 'reverse domain nucleation' in multidomain particles.) Such a model has been proposed for single-domain acicular particles, wherein a 180° domain wall forms at one end of the particle, then propagates to the other end, flipping spins as it goes [61]. Although experimental evidence for this model was drawn from microscopic observations on single particles, and measurements on very dilute suspensions [62], it has not yet been validated [53].

A significant proportion of current theoretical research on the reversal mechanism in isolated particles is based on computer simulations [63]. An illustration of this is given in figure 6, which shows the magnetization reversal in a cubic particle of dimension 50 nm × 50 nm × 50 nm, in which the volume is divided into 6 × 6 × 6 cubic elements [64]. In common with all calculations of this type, the magnetization in each element is assumed to be constant, but the magnetization direction is allowed to vary from element to element. Such simulations have recently been used to elucidate the effect of both shape and crystalline anisotropy on reversal mechanisms [64], to model the switching process in both acicular γ-Fe_2O_3 particles [65] and in Co-surface-modified γ-Fe_2O_3 [66, 67], and to predict the effect of shape defects on the reversal mechanism in hexagonal platelet particles such as Co–Ti-substituted barium ferrite [68].

3.1.2. Particle assemblies. Whereas the magnetization reversal process in isolated particles is reasonably well understood, it is considerably more difficult to quantitatively understand the same process in a macroscopic sample containing many fine particles. Not only do the particles have variable shape and dimension, but there is also a distribution of easy anisotropy directions and the likelihood of significant magnetostatic interparticle interactions—all of which are factors that affect the observed response to the applied field. As illustrated in figure 7, one obtains a hysteresis curve that comprises contributions from the constituent single-domain particles, and a distribution of switching fields rather than the unique switching field of a single isolated particle.

In the absence of interparticle interactions, the magnetic response of an assembly of single-domain particles is governed by both the character of the system (distributions in

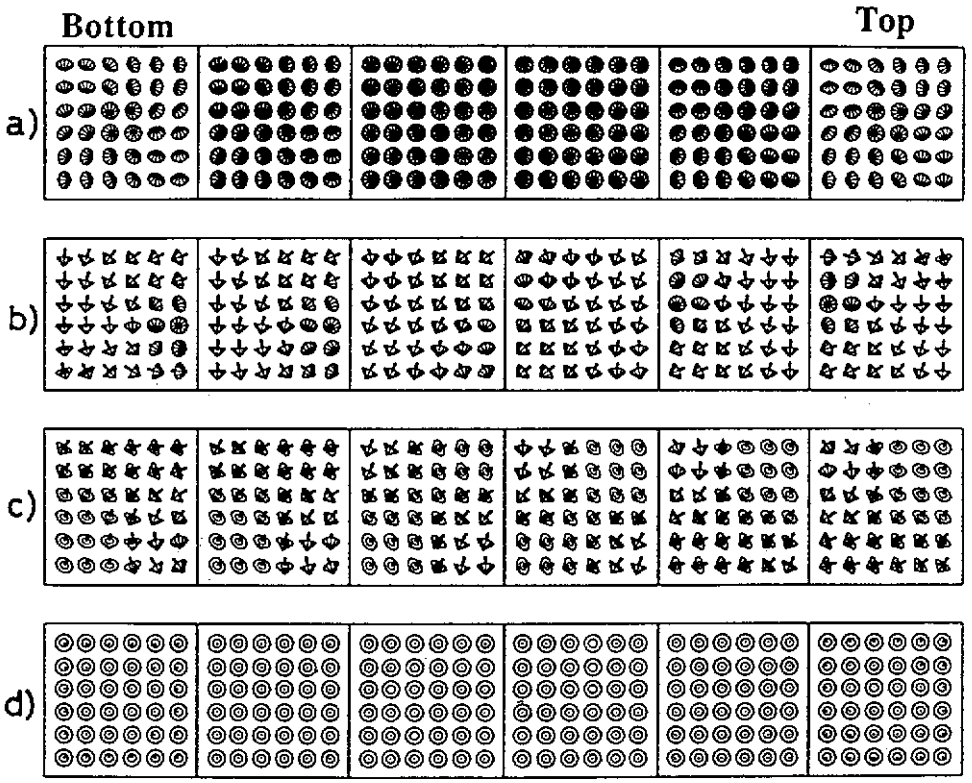

Figure 6. Computer simulation of magnetization reversal in a cubic particle. A uniaxial anisotropy of 1.96×10^4 J m^{-3} was assumed, and the 50 nm × 50 nm × 50 nm particle was divided into $6 \times 6 \times 6$ elements. An applied field of intensity -111 kA m^{-1} (-1395 Oe in cgs units) was introduced at time $t = 0$. The magnetic states are shown for (a) $t = 0.5$ ns, (b) $t = 4.68$ ns, (c) $t = 4.73$ ns and (d) $t = 5$ ns. This figure is reproduced with permission from [64].

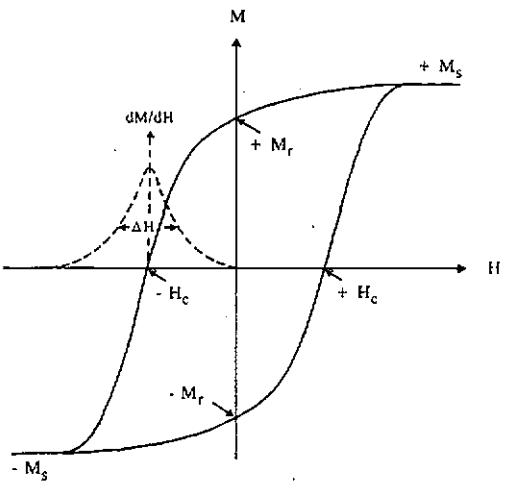

Figure 7. Hysteresis loop in an assembly of particles, showing the coercivity H_c, remanent magnetization M_r, and saturation magnetization M_s. Also shown is the switching field distribution curve, dM/dH versus H, which may be characterized by the parameter $S = \Delta H/H_c$.

particle size, morphology, anisotropy, and texture) and by external parameters such as the applied field strength and temperature. The shape and anisotropy of the individual particles affect the coercivities of the particles. Particle size also affects the coercivity: in larger particles there is a tendency toward multidomain magnetic structures, with a resultant drop in coercivity. In smaller particles the coercivity again falls as the result of the increasing effect of thermal agitation on the particle magnetization—as the particle size decreases this eventually leads to zero coercivity and 'superparamagnetism', as the net moment on the particle behaves as a paramagnet. Similarly, the orientational texture of the assembly affects the observed response, since the coercivity depends on the angle between the applied field and the easy anisotropy axis, as illustrated in figure 5.

Recent theoretical research on non-interacting assemblies has shown that particle size distributions and orientational texture may strongly influence observed parameters such as the switching-field distribution [29, 69]. Experimental work falls into two categories: model systems and low-field data. In model systems highly diluted particle assemblies are prepared so that the interparticle distances are large, and interaction effects are minimized. Examples of such systems are frozen magnetic fluids having volume fractions of less than 2% magnetic material, used to test the Néel model of superparamagnetic relaxation [70], and γ-Fe_2O_3 particles dispersed in gradually hardening epoxy resin (volume fraction $\sim$ 0.03%), used to study field-induced anisotropy in magnetic recording tape particles [71]. In the second category of experiment very small measuring fields, much smaller than the anisotropy field, are used to measure quantities such as the initial susceptibility of the system. It is then assumed that the response approximates that of an assembly of isolated particles.

Magnetostatic interparticle interactions, particularly the long-range dipole–dipole interactions, are significant contributors in determining the magnetic response of many fine-particle systems, such as high-density recording media dispersions. Broadly speaking there are three different approaches to the theoretical modelling of such interactions: phenomenological, mean field, and micromagnetic.

The most popular model that allows interparticle interactions was introduced by Preisach in 1935 to model hysteresis [72]. In the Preisach model the overall response is described by the superposition of many elementary asymmetric square hysteresis loops, with a density function determining the relative contribution of each elementary loop. The asymmetry in the elementary loops (different switching fields H_+ and H_- in the positive and negative directions) is used to introduce the interaction effects. There are many variants on the Preisach model, including the 'product', 'moving', and 'vector' Preisach models. Most recently, the 'vector moving' Preisach model has been developed, wherein the total magnetization of the medium is computed by multiplying the scalar Preisach density function by a process-dependent vector function [73]. This model has been shown to agree well with the observed magnetic properties in several γ-Fe_2O_3 and Co-adsorbed γ-Fe_2O_3 particle assemblies [74].

In mean-field and micromagnetic models the emphasis is on incorporating known physical principles into the model to predict the behaviour of the system. An example of the techniques used in mean-field models is the method of convoluting a local interaction field density distribution with the predicted behaviour of an ideal non-interacting ensemble, to model the interaction effects [75]. Another technique, used for multidomain particles, is to assume that the moments in each domain interact with the applied field and with a weighted mean of the bulk magnetization [76]. In micromagnetic models the details of the interactions are taken into account explicitly, on a microscopic scale. Both numerical and analytical methods are used. Examples of the numerical approach include Monte Carlo simulations of the noise in recording media [77], and work based on finite arrays of moments in the presence

of explicitly defined interaction energy constraints [78, 79]. Analytical formulations have been applied to some specific systems, such as infinite samples containing finite clusters of up to four interacting particles, with no interactions between neighbouring clusters [80].

Experimental research on magnetostatic interactions in particle assemblies is largely based on comparative measurements of two remanence curves: the DC demagnetization curve $I_d(H)$, and the isothermal remanent magnetization curve $I_r(H)$†. The $I_d(H)$ curve is measured by initially saturating the sample in the positive direction, then successively applying and removing progressively larger fields in the negative direction, recording the remanence at each step. The $I_r(H)$ curve is measured similarly, except that the system is initially in an AC demagnetized state. Typical (normalized) I_d and I_r curves are shown in figure 8. In 1958, Wohlfarth [81] showed that in an assembly of non-interacting single-domain particles, the relation

$$I_d(H) = I_r(\infty) - 2I_r(H) \tag{1}$$

should hold, irrespective of any texture or anisotropy distributions in the sample. Consequently, any deviation from such a linear relation between the two remanence curves may be attributed to the effect of interparticle interactions.

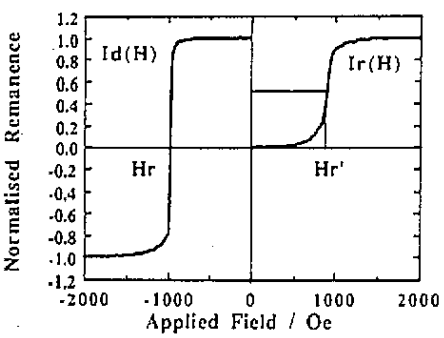

Figure 8. Typical examples of the DC demagnetization curve $I_d(H)$ and the isothermal remanent magnetization curve $I_r(H)$. This figure is reproduced with permission from [84].

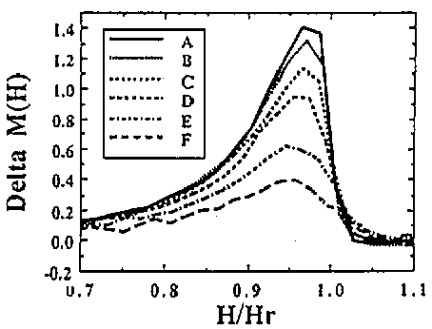

Figure 9. 'Δ plot' for quantifying interparticle interaction effects in a series of barium ferrite samples that differ only in their volumetric packing densities. Samples A–F have packing densities of 35%, 34%, 33%, 30%, 23%, and 10% respectively. This figure is reproduced with permission from [84].

Two parameters have been used to quantify the strength of the interactions, based on the remanence curves. These are the 'interaction-field factor' [82]

$$\text{IFF} = (H_r' - H_r)/H_c \tag{2}$$

where H_r and H_r' are the remanence fields defined in figure 8 and, more recently, the 'Δ plot' [83], which comprises the curve

$$\Delta I(H) = I_d(H) - [I_r(\infty) - 2I_r(H)]. \tag{3}$$

† In the SI Sommerfield system $B = \mu_0(H + M)$, whereas the common use of $I = \mu_0 M$ as the magnetic polarization is the Kennelly convention. These definitions are not mutually exclusive.

Using these parameters, researchers have followed the evolution in magnetic interactions as a function of numerous variables, such as the volumetric packing density [84] and particle size [85] in barium ferrite samples, and the packing density and surface coating of γ-Fe_2O_3 particles [86, 87]. An illustration of the results obtained by such methods is the 'Δ plot' shown in figure 9, which shows the increase in strength of the interparticle interactions as the packing density is increased [84].

3.2. Surface effects

As the physical dimensions of a particle decrease, the proportion of those magnetic ions that are at or near the surface of the particle increases. Fine particles therefore provide an opportunity to measure effects not observed in the corresponding bulk materials. Similarly, the act of coating the surfaces of fine particles may significantly alter the magnetic properties of the system. The identification and elucidation of such effects is the subject of much contemporary research.

Surface phenomena have been studied in a wide range of fine-particle magnetic oxides, including a haematite [88, 89] and barium ferrite [90]. However, over the last two decades one material in particular has been extensively investigated, viz. the magnetic recording medium maghemite (γ-Fe_2O_3), in both its untreated and surface-modified forms [91–93]. This interest is partly due to the discovery, in the early 1970s, of a method of significantly enhancing the coercivity of acicular γ-Fe_2O_3 particles by adsorbing Co^{2+} ions onto the surface of the particles [94]. This increased coercivity promoted the development of high-density recording media, and Co-modified maghemite is now common in video and audio tapes. Despite the huge commercial importance of these materials, the mechanism by which the surface treatment increases the coercivity is not well understood, and continues to be the subject of controversy.

One aspect of the research on Co-modified maghemite concerns the nature of the surface anisotropy. When Co is adsorbed onto acicular maghemite particles, the uniaxial anisotropy of the precursor material, which is predominantly due to shape anisotropy, is retained and strengthened. This is surprising, since the volume doping of Co ions into the interior of maghemite particles introduces a multiaxial anisotropy associated with the large single-ion anisotropy of the Co^{2+} ion [95]. Also, the outermost atomic layers of the Co-modified particles are believed to contain, for the most part, epitaxially oriented cobalt ferrite ($CoFe_2O_4$) [96, 97], and as such would be expected to have easy anisotropy axes that were not collinear with those of the interior [27]. Various explanations have been given to account for the observed uniaxial anisotropy. It has been suggested that the demagnetization field of the particle maghemite core influences the formation of a uniaxial cobalt ferrite coating, either by establishing a preferred orientation for the Co^{2+} ions or for the $CoFe_2O_4$ microcrystals, or by favouring a migration of the Co^{2+} ions to lattice sites with symmetry axes close to the field direction [97–99]. Alternatively, it has been proposed that the surface $CoFe_2O_4$ crystallites are imperfectly formed, reducing their intrinsic magnetocrystalline anisotropy, and allowing the particle shape anisotropy to dominate [100]. It is not yet clear which of these models is most appropriate.

In related work, a quantum mechanism has been proposed to account for an increase in the surface anisotropy of partially reduced maghemite, in which a modest proportion of Fe^{2+} ions are present [101]. In essence, the anisotropy is associated with the spin–orbit energy of electrons in 3d ε orbitals around Fe^{3+} cores near the crystal surface. This theory may help to explain the origin of the increased coercivity seen in partially reduced γ-Fe_2O_3 following surface treatment with aqueous sodium polyphosphate, $(NaPO_3)_n.Na_2O$ [102, 103].

In experimental studies of the microscopic magnetic properties of both untreated and surface-modified maghemite particles, applied-field Mössbauer spectroscopy has been frequently employed to great effect [104–109]. Attention has centred on the so-called 'spin-canting anomaly', where, even in large applied fields (up to 10 T), there is significant canting of the Fe^{3+} atomic moments away from the applied field direction. The magnetization of the particles is apparently not completely saturated by the applied field—an effect that has been confirmed from magnetization measurements [110, 111]. Early researchers attributed this to a pinned, non-collinear spin structure for the surface moments, independent of the interior of the particle where the moments were thought to be collinear with the applied field. This view was supported by observations that the canting effect in maghemite increased with decreasing particle size, and also increased when the particles were coated with the Mössbauer-specific isotope ^{57}Fe [106].

However, more recent work has provided data which do not support this model. Detailed examination of the applied-field Mössbauer spectra of maghemite particles similar to those used in the earlier experiments revealed the presence of a small amount of α-Fe_2O_3 impurity [107]. These data are shown in figure 10. Given that the contributions of any haematite impurities are only clearly apparent in fields of 6 T or more and when high-quality spectra are collected, they may have gone unnoticed in earlier experiments, thereby confounding both the measurements and the inferences reported.

Subsequently, the spin-canting effect in Co-adsorbed maghemite particles (containing no α-Fe_2O_3 impurities) has been analysed in terms of the approach to saturation of an assembly of particles undergoing coherent magnetization reversal, as described by the Stoner–Wohlfarth model [108, 112]. It was found that this model, which makes no distinction at all between the responses of the interior and surface moments, gave adequate results provided a relatively high uniaxial anisotropy term was allowed, i.e. an anisotropy field of the order of 1 T, corresponding to an anisotropy constant $K_1 \simeq 5 \times 10^5$ J m^{-3} [113]. The measured anisotropy in Co–maghemite particles is usually of the order of $1–2 \times 10^4$ J m^{-3}. The significance of this discrepancy is yet to be resolved, although it may be a consequence of the assumption of a coherent reversal mechanism—in early work using such a model, anisotropies as high as 3×10^6 J m^{-3} were reported [105].

In another study, the applied-field Mössbauer spectra of a series of selectively coated maghemite particles were found to be inconsistent with the surface spin-canting model [109]. A 'ferrimagnetic-chain' model was proposed, in which a high-anisotropy (2.3×10^5 J m^{-3}) $CoFe_2O_4$ shell effectively pins the end ions of a chain of magnetically coupled Fe^{3+} sublattice ions, resulting in a parabolic dependence of the spin angle as a function of lattice position. This model is similar to micromagnetic models of Co-adsorbed maghemite where the particle volume is divided into a low-anisotropy inner core and a high-anisotropy shell region [63, 67]. One intriguing result of the numerical modelling thus performed is that if there is an appreciable angle θ between the easy anisotropy axis and the applied field direction, the magnetization processes in the core are more uniform than they would be if the applied field was collinear with the anisotropy axis. In particular, for θ values of the order of 70–90°, the magnetization reversal proceeds by an almost uniform rotation, and the magnetization switching field is determined mainly by the anisotropy of the shell region [63]. This may be an important factor in explaining the Mössbauer results, especially the unexpected success of the simple Stoner–Wohlfarth model, given that the observed spin-canting effects are largely attributed to those particles whose easy anisotropy axes lie most nearly perpendicular to the applied field [108].

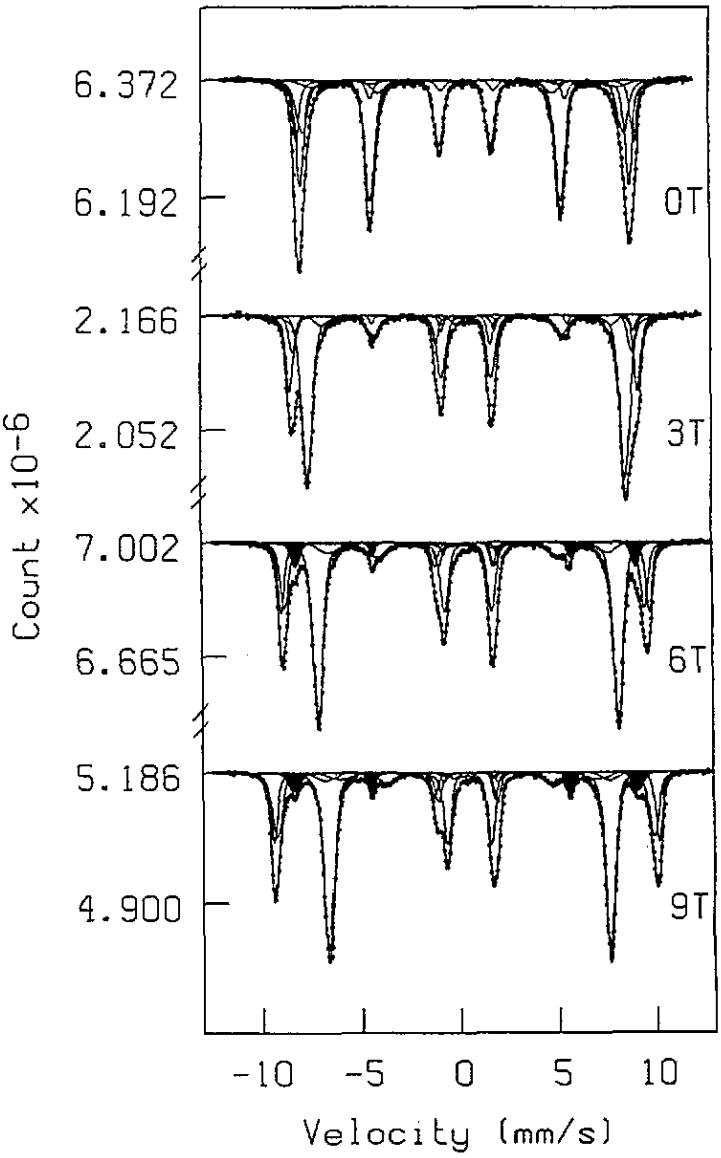

Figure 10. ^{57}Fe Mössbauer spectra of maghemite (γ-Fe_2O_3) particles at 4.2 K in applied fields of 0, 3, 6, and 9 T directed parallel to the γ-ray beam. The particles are acicular, being 350 nm long and with an axial ratio of about 4.8:1. An impurity component (the shaded subspectrum) becomes evident in the high-field spectra, and is identified as haematite, α-Fe_2O_3.

3.3. Intrinsic properties

There are many fundamental questions relating to the intrinsic magnetic properties of fine particles. Examples include the nature of the equilibrium micromagnetic structure of single-domain ferrimagnetic particles [114], and the origin of the reduced saturation magnetization and increased coercivity observed in ferrite and iron oxide particles of less than 20 nm in size [115, 116]. A detailed description of all such research topics is beyond the scope of

this article, and we restrict the discussion to several issues that have received attention in the literature recently.

3.3.1. Structural and magnetic disorder. The effects of structural and magnetic disorder on the magnetic properties of fine particles are frequently encountered in naturally occurring materials, such as soil-related iron oxides and oxyhydroxides [117, 118]. We consider two topics related to the effects of disorder: the appearance of a weak net magnetic moment in small antiferromagnetic particles, and the magnetic ground state of disordered insulators.

Over thirty years ago Néel postulated that in very small antiferromagnetic particles an 'uncompensated' net moment could appear as the result of the unequal occupation of the spin-up and spin-down sublattices [119]. He suggested that the number of uncompensated moments in a particle containing N moments would be of the order of $N^{1/2}$, giving a net moment per magnetic atom of order $N^{-1/2}$—a negligible amount unless N is small†. Subsequently, weak moments were observed in naturally occurring particles of the antiferromagnet goethite (α-FeOOH) [120, 121]. The strength of the moment increased both with decreasing particle size and with increasing amounts of Al^{3+} ion impurities in the lattice. The magnitude of the moment exceeded that predicted by Néel, and it was proposed that vacancies, defects, and (for aluminous goethites) a preferential occupation of the diamagnetic Al^{3+} ions on one of the two Fe^{3+} sublattices, were responsible for the observed moment [121].

Alternative explanations have been put forward, such as one involving structural defects and associated surface effects [122]. However, this explanation underestimates the observed moment. The most recent applied-field experiments and analyses have been found to support the non-random aluminium substitution hypothesis [123], although the mechanism causing this preference is unknown.

Another intriguing issue is the magnetic ground state in amorphous or disordered insulators. Some years ago applied-field Mössbauer-effect measurements on an amorphous insulator, a gelatinous material that consisted of fine particles of $Fe(OH)_3.0.9H_2O$ in an organic matrix, led to the proposed existence of a new type of magnetic order, termed 'speromagnetism' [124]. In speromagnets, the spin arrangement on an atomic nearest-neighbour level is disordered, with the moment directions isotropically distributed over a sphere, despite the presence of strong antiferromagnetic exchange interactions. Recently it has been suggested that it is difficult or impossible to use applied-field Mössbauer spectroscopy to distinguish between random spin structures on an atomic level (as in a speromagnet) and random structure at the level of domains, crystallites, and particles (as in a disordered, but essentially crystalline system) [125, 126]. Consequently, there is now continuing and vigorous debate over the existence or otherwise of the speromagnetic state in insulators [113, 127].

3.3.2. Superparamagnetism. In sufficiently small ferromagnetic or ferrimagnetic single-domain particles, the anisotropy energy barrier to magnetization reversal may be small enough for thermal agitation to flip the magnetization direction back and forth between equivalent energy minima. This phenomenon is known as superparamagnetism. Although it is intuitively reasonable that the relaxation rate for these reversals will vary exponentially

† A justification for this proposed proportionality comes from a statistical 'random-walk' argument. If the moments at each lattice site have one degree of freedom (i.e. may be either spin up or spin down), the random occupation of those sites gives a net moment of $0.79N^{1/2}$. If the moments have two degrees of freedom (i.e. are confined to a plane), this becomes $0.89N^{1/2}$, while for three degrees of freedom the predicted moment is $0.92N^{1/2}$.

with temperature, the precise quantitative description of the process is complex, and is not yet fully understood.

The classical theory of the relaxation process was first considered many years ago by Néel [128] and then by Brown [129,130]. These two models, which continue to be used, have recently been critically compared [131,132]. Néel equated a vibrational fluctuation energy to the thermal energy $k_B T$, and derived an expression for the relaxation time τ for the magnetization reversal. Assuming a uniaxial anisotropy constant K and particles of volume V, Néel obtained

$$\tau_N^{-1} = \gamma H_c |3G\lambda + DM_s^2| [\alpha/(\pi GK)]^{1/2} e^{-\alpha} \tag{4}$$

where G is the Young's modulus, λ the magnetostriction, D the demagnetization factor, M_s the magnetization, γ the gyromagnetic ratio, $H_c = 2K/M_s$, and $\alpha = KV/k_B T$. This expression is often written in the simplified form $\tau_N^{-1} = \tau_o^{-1} e^{-\alpha}$, where τ_o is taken to be a constant preexponential factor. In a different approach, Brown equated a magnetic fluctuation energy to $k_B T$, and derived a Fokker–Planck differential equation to describe the 'random walk' of the magnetization direction from one energy minimum to another. Although Brown did not solve the differential equation, he showed that under critical damping the result was

$$\tau_B^{-1} = \tfrac{1}{2} \gamma H_c (\alpha/\pi)^{1/2} e^{-\alpha}. \tag{5}$$

Brown also showed that for 30 nm diameter particles $\tau_B \simeq \tau_N$, and that the preexponential factors in both expressions lie in the range 10^{10}–10^{12} s^{-1} [130].

It has been suggested that of the two models it is the less sophisticated Néel model that gives more physically reasonable results for particles of less than 10^6 atoms [131], but that the Brown model has the distinct advantage of being applicable to non-uniaxial systems [132]. Theoretical work continues. For example, analytical expressions were recently obtained for the eigenvalues of Brown's Fokker–Planck equation, both in zero field [133] and in applied fields [134]. However, a good deal of work is needed before a comprehensive quantitative understanding of superparamagnetism is achieved, particularly if, as suggested, other factors such as quantum fluctuations are more important in the relaxation process than has been previously thought [131].

Experimentally, superparamagnetism may be observed by a variety of techniques, including neutron scattering, Mössbauer spectroscopy, magnetization, and susceptibility measurements. Each method has a characteristic measurement time, ranging from $\sim 10^{-14}$–10^{-12} s for neutron scattering to ~ 10 s for bulk measurements, and is therefore sensitive to different relaxation rates. However, the majority of studies of superparamagnetism in fine particles have used the Mössbauer technique, as its measurement time (the Larmour precession frequency) of $\sim 10^{-8}$ s leads to critical phenomena at convenient temperatures (typically 20–300 K) and because the presence of Fe makes many fine-particle samples amenable to Mössbauer investigations. Applied-field experiments performed both above and below the critical temperature provide information about the anisotropy and magnetization of the particles [135], and have been used to infer the presence of interparticle magnetic interactions [136].

However, most recently Bocquet and coworkers studied a synthetic sample of fine goethite particles using neutron diffraction, Mössbauer spectroscopy and magnetization measurements [137]. Surprisingly, the three methods gave the same magnetic ordering temperature: it was 358 ± 1 K, compared to nearly 400 K for the bulk material. It was

concluded that because the measurement times of the three techniques vary by many orders of magnitude, superparamagnetism could not be present. The characteristic line broadening observed in Mössbauer spectra, and hitherto analysed in terms of superparamagnetism, was interpreted in terms of magnetically ordered clusters created by high concentrations of vacancy defects [138]. At certain temperatures the cluster moments slowly relax, producing a Boltzmann distribution of the magnetization. This model provides excellent fits to the temperature-dependent hyperfine-field distributions observed in Mössbauer spectra.

3.3.3. Quantum tunnelling of magnetization. We conclude this section with a topic that has received considerable attention over the last few years, viz. macroscopic quantum tunnelling in magnetic fine particles. The theoretical basis for this work was proposed in 1988 by Chudnovsky and Gunther [139], with a model that allowed prediction of the rate of quantum switching in a single-domain ferromagnetic particle. Possible experimental situations in which such quantum effects might be observable were also suggested. In 1990 the model was extended to single-domain antiferromagnetic particles [140, 141], and much larger effects, observable at temperatures of the order of a few kelvin, were predicted.

Initial SQUID susceptibility experiments on nanometre-scale FeCO particles were suggestive of quantum effects, but were inconclusive [142]. Later magnetic relaxation measurements on 15 nm particles of ferromagnetic $Tb_{0.5}Ce_{0.5}Fe_2$ gave a clear indication of a crossover between thermal activation and quantum-tunnelling regimes at ~ 1.2 K [143]. Since then experimental evidence for quantum effects has been observed in several systems, mainly metallic clusters such as those found in thin-film alloys of Fe–Sm [144], but also materials such as FeC magnetic fluids [145] and the ferrihydrite cores of the magnetic protein ferritin (approximate formula $5Fe_2O_3.9H_2O$) [146]. It remains to be seen what implications this research may have for applications of magnetic materials—it has been suggested that quantum switching effects place an upper limit on the lifetime of high-density magnetic recording media.

4. Conclusions

We have given an overview of the magnetic properties of fine-particle oxides in the context of current research and development. The special requirements of fine particles for use in devices such as magnetic fluids, magnetic separators and flocculators, magnetic recording media, and biomagnetometers have been discussed. The many and varied uses to which fine-particle oxides are put is testimony to the value of single-domain ferrimagnetic particles with dimensions on the micrometre or nanometre scale. Among the various avenues of research on fine-particle magnetism we have highlighted work on magnetization reversal mechanisms in isolated particles and in particle assemblies, magnetostatic interparticle interactions, surface effects, structural disorder, superparamagnetism, and quantum tunnelling. The diversity of these topics indicates the rich veins of as-yet unexplored physical characteristics and properties of fine-particle systems.

The combination of technological relevance and fundamental questions regarding the underlying physical behaviour should ensure that the high level of current research on fine-particle magnetic oxides will continue.

References

[1] Charles S W 1987 *J. Magn. Magn. Mater.* **65** 350–7

[2] Anton I, De Sabata I and Vékás L 1990 *J. Magn. Magn. Mater.* **85** 219–26
[3] Raj K and Moskowitz R 1990 *J. Magn. Magn. Mater.* **85** 233–45
[4] Sakurai T, Inoue T, Munakata M and Goto K 1988 *IEEE Transl. J. Magn. Japan* **3** 504–5
[5] Rice P and Moreland J 1991 *Rev. Sci. Instrum.* **62** 844–5
[6] Goebbels K 1988 *Materialpruefung* **30** 327–32
[7] Henning D and Walther K G 1988 *Mater. Eval.* **46** 1588–91
[8] Wong B S 1990 *Br. J. Non-Destruct. Testing* **32** 303–7
[9] Wills B A 1985 *Mineral Processing Technology* (Oxford: Pergmanon) ch 13
[10] Oberteuffer J A 1974 *IEEE Trans. Magn.* **MAG-10** 223–38
[11] Kolm H H 1975 *IEEE Trans. Magn.* **MAG-11** 1567–9
[12] Oder R R 1976 *IEEE Trans. Magn.* **MAG-12** 429–35
[13] Gerber R 1982 *IEEE Trans. Magn.* **MAG-18** 812–6
[14] Moyer C, Natenapit M and Arajs S 1986 *J. Magn. Magn. Mater.* **54–7** 1475–7
[15] Haque M F, Aidun R, Moyer C and Arajs S 1988 *J. Appl. Phys.* **63** 3239–40
[16] Kopp J 1983 *Int. J. Mineral Processing* **10** 297–308
[17] Boehm J, Fletcher D and Parker M R 1986 *IEEE Trans. Magn.* **MAG-22** 1122–4
[18] Turner J M, Parker M R and Fletcher D 1988 *IEEE Trans. Magn.* **MAG-24** 866–9
[19] Cheremynkh P A, Fedorov V K, Klimenko E Y, Lunin V N and Novikov S I 1988 *IEEE Trans. Magn.* **MAG-24** 882–4
[20] Rosensweig R E 1985 *Ferrohydrodynamics* (Cambridge: Cambridge University Press)
[21] Resnick W, Zimmels Y and Boadi D 1988 *IEEE Trans. Magn.* **MAG-24** 757–60
[22] Harel O, Resnick W and Zimmels Y 1990 *J. Magn. Magn. Mater.* **83** 498–500
[23] Parker M R, van Kleef R P A R, Myron H W and Wyder P 1982 *J. Magn. Magn. Mater.* **27** 250–6
[24] Camras M 1985 *Magnetic Tape Recording* (New York: Van Nostrand Reinhold)
[25] Mee C D 1964 *The Physics of Magnetic Recording* (Amsterdam: North-Holland)
[26] Mallinson J C 1976 *IEEE Proc.* **64** 196–208
[27] Berkowitz A E 1986 *IEEE Trans. Magn.* **MAG-22** 466–71
[28] Sharrock M P 1989 *IEEE Trans. Magn.* **MAG-25** 4374–89
[29] Chantrell R W 1989 *Textures Microstruct.* **11** 107–25
[30] O'Grady K, Gilson R G and Hobby P C 1991 *J. Magn. Magn. Mater.* **95** 341–55
[31] Bate G 1991 *J. Magn. Magn. Mater.* **100** 413–24
[32] Suzuki T 1984 *IEEE Trans. Magn.* **MAG-20** 675–80
[33] Kirschvink J L 1989 *Bioelectromagnetism* **10** 239–59
[34] Frankel R B, Blakemore R P and Wolfe R S 1979 *Science* **203** 1355–6
[35] Kirschvink J L, Kobayashi-Kirschvink A and Woodford B J 1992 *Proc. Natl Acad. Sci. USA* **89** 7683–7
[36] Futschik K, Pfutzner H, Doblander A, Schonhuber P, Dobeneck T, Petersen N and Vali H 1989 *IEEE Eng. Med. Biol. Magn.* **EMBM-8** 46–7
[37] Funaki M, Sakai H and Matsunaga T 1989 *J. Geomagn. Geoelect.* **41** 77–87
[38] Bahaj A S, Watson J H P and Ellwood D C 1980 *IEEE Trans. Magn.* **MAG-25** 3809–11
[39] Bahaj A S, Ellwood D C and Watson J H P 1991 *IEEE Trans. Magn.* **MAG-27** 5371–4
[40] Matsunaga T and Kamiya S 1987 *Appl. Microbiol. Biotechnol.* **26** 328–32
[41] Saini S, Ferrucci J T, Stark D D and Wittenberg J 1986 *Gastron. Radiol.* **11** 296
[42] Cerdan S, Lotscher H R, Kunnecke B and Seelig J 1989 *Magn. Reson. Med.* **12** 151–63
[43] Ugelstad J, Berge A and Ellingsen T 1987 *Bone Marrow Transplant.* **2** 74–7
[44] Sato S B, Ohnishi S, Sako Y and Yamashina S 1986 *J. Biochem.* **100** 1481–92
[45] Kvalheim G, Fodstad O, Funderud S, Nustad K, Pharo A, Pihl A and Ugelstad A 1987 *J. Cancer Res.* **47** 846–51
[46] Mavrichev A S and Fertman V Y 1991 *Voprosy Onkol.* **37** 11–7
[47] Birkmeyer R C, Diaco R, Hutson D K, Lau H P, Miller W K, Neelkantan N V, Pankratz T J, Tseng S Y, Vickery D K and Yang E K 1987 *Clin. Chem.* **33** 1543–7
[48] Charles S W 1990 *J. Magn. Magn. Mater.* **85** 277–84
[49] Roath S, Smith A R and Watson J H P 1990 *J. Magn. Magn. Mater.* **85** 285–9
[50] Takemori S, Tazawa K, Nagae H, Shimizu T, Masuko Y, Okamoto M and Fujimaki M 1992 *Gan to Kagaku Ryoho* **19** 1648–50
[51] Mizutani H, Suzuki M, Mizutani H, Fujiwara K, Shibata S, Arishima K, Hoshino M, Ushijima H, Honma H and Kitamura T 1991 *Microbiol. Immunol.* **35** 717–27
[52] Valberg P A and Butler J P 1987 *Biophys. J.* **52** 537–50
[53] Aharoni A 1986 *IEEE Trans. Magn.* **MAG-22** 478–88
[54] Della Torre E 1986 *IEEE Trans. Magn.* **MAG-22** 484–9

[55] Della Torre E 1990 *Proc. IEEE* **78** 1017–26
[56] Stoner E C and Wohlfarth E P 1948 *Phil. Trans. R. Soc.* A **240** 599–642
[57] Jacobs I S and Bean C P 1955 *Phys. Rev.* **100** 1060–7
[58] Aharoni A 1966 *Phys. Status Solidi* **16** 3–42
[59] Kuo P C 1988 *J. Appl. Phys.* **64** 5071–83
[60] Ishii Y and Sato M 1986 *J. Appl. Phys.* **59** 880–7
[61] Knowles J E 1986 *J. Magn. Magn. Mater.* **61** 121–8
[62] Knowles J E 1984 *IEEE Trans. Magn.* **MAG-20** 84–6
[63] Schabes M E 1991 *J. Magn. Magn. Mater.* **95** 249–88
[64] Spratt G, Uesaka Y, Nakatani Y and Hayashi N 1991 *J. Appl. Phys.* **69** 4850–2
[65] Schabes M E and Bertram H N 1988 *J. Appl. Phys.* **64** 5832–4
[66] Aharoni A 1988 *J. Appl. Phys.* **63** 4605–8
[67] Schabes M E and Bertram H N 1990 *J. Appl. Phys.* **67** 5149–51
[68] Uesaka Y, Nakatani Y and Hayashi N 1991 *J. Appl. Phys.* **69** 4847–9
[69] Chantrell R W, O'Grady K, Bradbury A, Charles S W and Hopkins N 1987 *IEEE Trans. Magn.* **MAG-23** 204–6
[70] Bacri J C, Perzynski R and Salin D 1988 *J. Magn. Magn. Mater.* **71** 246–54
[71] Potter D K and Stephenson A 1988 *J. Appl. Phys.* **63** 1691–3
[72] Preisach F 1935 *Z. Phys.* **94** 277–302
[73] Oti J and Della Torre E 1990 *J. Appl. Phys.* **67** 5364–6
[74] Vajda F, Oti J, Pardavi-Horvath M, Della Torre E, Swartzendruber L J and Bennett L H 1991 *J. Appl. Phys.* **69** 4502–4
[75] Berkov D V 1991 *J. Magn. Magn. Mater.* **101** 221–3
[76] Jiles D C and Atherton D L 1986 *J. Magn. Magn. Mater.* **61** 48–60
[77] Arratia R A and Bertram H N 1984 *IEEE Trans. Magn.* **MAG-20** 412–20
[78] Lyberatos A, Wohlfarth E P and Chantrell R W 1985 *IEEE Trans. Magn.* **MAG-21** 1277–82
[79] Rekveldt M T and Rosman R 1991 *J. Magn. Magn. Mater.* **95** 221–30
[80] Christoph V and Elk K 1988 *J. Magn. Magn. Mater.* **74** 143–8
[81] Wohlfarth E P 1958 *J. Appl. Phys.* **29** 595–6
[82] Corradi A R and Wohlfarth E P 1978 *IEEE Trans. Magn.* **MAG-14** 861–3
[83] Kelly P E, O'Grady K, Mayo P I and Chantrell R W 1989 *IEEE Trans. Magn.* **MAG-25** 3880–3
[84] Spratt G W D, Kodama N, Inoue H, Uesaka Y and Katsumoto M 1991 *IEEE Trans. Magn.* **MAG-27** 4661–3
[85] El Hilo M, O'Grady K and Chantrell R W 1991 *IEEE Trans. Magn.* **MAG-27** 4666–8
[86] Bottoni G 1991 *J. Appl. Phys.* **69** 4499–501
[87] Bottoni G, Candolfo D, Cecchetti A and Masoli F 1992 *J. Magn. Magn. Mater.* **104–7** 975–6
[88] Shinjo T, Kiyama M, Sugita N, Watanabe K and Takada T 1983 *J. Magn. Magn. Mater.* **35** 133–5
[89] Wang G H, Zhong X P, Wang Q, Luo H L and Hou D L 1991 *J. Appl. Phys.* **70** 5906–8
[90] Kurisu S, Ido T and Yokoyama H 1987 *IEEE Trans. Magn.* **MAG-23** 3137–9
[91] Mularie W M and Sharrock M P 1991 *J. Appl. Phys.* **69** 4938–41
[92] Berkowitz A E 1991 *Science and Technology of Nanostructured Magnetic Materials* ed G C Hadjipanayis and G A Prinz (New York: Plenum) pp 533–44
[93] Berkowitz A E, Parker F T, Spada F E and Margulies D 1992 *Magnetic Properties of Fine Particles* ed J L Dormann and D Fiorani (Amsterdam: Elsevier) pp 309–22
[94] Umeki S, Saitoh S and Imaoka Y 1974 *IEEE Trans. Magn.* **MAG-10** 655–6
[95] Köster E 1972 *IEEE Trans. Magn.* **MAG-8** 428–9
[96] Sumiya K, Matsumoto T, Watatani S and Hayama F 1979 *J. Phys. Chem. Solids* **40** 1097–102
[97] Sharrock M P, Picone P J and Morrish A H 1983 *IEEE Trans. Magn.* **MAG-19** 1466–73
[98] Kishimoto M, Kitaoka S, Andoh H, Amemiya M and Hayama F 1981 *IEEE Trans. Magn.* **MAG-17** 3029–31
[99] Lin Z 1992 *J. Magn. Magn. Mater.* **116** 147–53
[100] Zhang S G, Gao Z S, Jiang S T and Wu L X 1990 *IEEE Trans. Magn.* **MAG-26** 1149–52
[101] Slonczewski J C 1992 *J. Magn. Magn. Mater.* **117** 368–78
[102] Itoh F, Satou M and Yamazaki Y 1977 *IEEE Trans. Magn.* **MAG-13** 1385–7
[103] Spada F E, Berkowitz A E and Prokey N T 1991 *J. Appl. Phys.* **69** 4475–7
[104] Coey J M D 1971 *Phys. Rev. Lett.* **27** 1140–2
[105] Clark P E and Morrish A H 1973 *AIP Conf. Proc.* **18** 1412–6
[106] Morrish A H and Haneda K 1983 *J. Magn. Magn. Mater.* **35** 105–13
[107] Pollard R J 1990 *J. Phys.: Condens. Matter* **2** 983–91
[108] Pankhurst Q A and Pollard R J 1991 *Phys. Rev. Lett.* **67** 248–50
[109] Parker F T and Berkowitz A E 1991 *Phys. Rev.* B **44** 7437–43

[110] Berkowitz A E, Schuele W J and Flanders P J 1968 *J. Appl. Phys.* **39** 1261–63
[111] Mollard P, Germi P and Rousset A 1977 *Physica* B & C **86–8** 1393–4
[112] Pankhurst Q A 1991 *J. Magn. Magn. Mater.* **101** 291–2
[113] Pankhurst Q A and Pollard R J 1993 *J. Phys.: Condens. Matter* **5** 7301–6
[114] Usov N A and Peschany S E 1992 *J. Magn. Magn. Mater.* **110** L1–L5
[115] Sato T, Iijima T, Seki M and Inagaki N 1987 *J. Magn. Magn. Mater.* **65** 252–6
[116] Nunes A C and Yu Z C 1989 *J. Magn. Magn. Mater.* **78** 241–6
[117] Pollard R J, Cardile C M, Lewis D G and Brown L J 1992 *Clay Miner.* **27** 57–71
[118] De Grave E, de Bakker P M A, Bowen L H and Vandenberghe R E 1992 *Z. Pflanzenernähr. Bodenk.* **155** 467–72
[119] Néel L 1962 *J. Phys. Soc. Japan Suppl.* B-1 **17** 676–85
[120] Strangway D W, Honea R M, McMahon B E and Larson E E 1968 *Geophys. J. R. Astron. Soc.* **15** 345–59
[121] Hedley I G 1971 *Z. Geophys.* **37** 409–20
[122] Brož D, Šolcová A, Šubrt J, Sedlák B, Zounová F and Reiman S I 1989 *Acta Phys. Slov.* **39** 235–8
[123] Pollard R J, Pankhurst Q A and Zientek P 1991 *Phys. Chem. Miner.* **18** 259–64
[124] Coey J M D and Readman P W 1973 *Nature* **246** 476–8
[125] Pankhurst Q A and Pollard R J 1992 *Clays Clay Miner.* **40** 268–72
[126] Pollard R J and Pankhurst Q A 1992 *J. Phys.: Condens. Matter* **4** L317–23
[127] Coey J M D 1993 *J. Phys.: Condens. Matter* **5** 7297–300
[128] Néel L 1949 *Ann. Geophys.* **5** 99–136
[129] Brown W F 1959 *J. Appl. Phys.* **30** 130S–2S
[130] Brown W F 1963 *Phys. Rev.* **130** 1677–86
[131] Jones D H and Srivastava K P 1989 *J. Magn. Magn. Mater.* **78** 320–8
[132] Aharoni A 1992 *Magnetic Properties of Fine Particles* ed J L Dormann and D Fiorani (Amsterdam: Elsevier) pp 3–11
[133] Bessais L, Ben Jaffel L and Dormann J L 1992 *Phys. Rev.* B **45** 7805–15
[134] Dormann J L and Bessais L 1992 *Hyperfine Interact.* **70** 1109–12
[135] St. Pierre T G, Jones D H and Dickson D P E 1987 *J. Magn. Magn. Mater.* **69** 276–84
[136] Mørup S 1992 *Magnetic Properties of Fine Particles* ed J L Dormann and D Fiorani (Amsterdam: Elsevier) pp 125–34
[137] Bocquet S and Kennedy S J 1992 *J. Magn. Magn. Mater.* **109** 260–4
[138] Bocquet S, Pollard R J and Cashion J D 1992 *Phys. Rev.* B **46** 11 657–64
[139] Chudnovsky E M and Gunther L 1988 *Phys. Rev. Lett.* **60** 661–4
[140] Barbara B and Chudnovsky E M 1990 *Phys. Lett.* **145A** 205–8
[141] Krive I V and Zaslavskii O B 1990 *J. Phys.: Condens. Matter* **2** 9457–62
[142] Awschalom D D, McCord M A and Grinstein G 1990 *Phys. Rev. Lett.* **65** 783–6
[143] Paulsen C, Sampaio L C, Barbara B, Fruchard D, Marchand A, Tholence J L and Uehara M 1991 *Phys. Lett.* **161A** 319–22
[144] Zhang X X, Balcells L, Ruiz J M, Tholence J L, Barbara B and Tejada J 1992 *J. Phys.: Condens. Matter* **4** L163–8
[145] Balcells Ll, Tholence J L, Linderoth S, Barbara B and Tejada J 1992 *Z. Phys.* B **89** 209–12
[146] Awschalom D D, Smyth J F, Grinstein G, DiVincenzo D P and Loss D 1992 *Phys. Rev. Lett.* **68** 3092–5